

<sup>10</sup> Korotkov, A. I., Sulimov, A. A., Obmenin, A. V., Dubovitskii, V. F., and Kurkin, A. I., "Transition of Burning to Detonation in Porous Explosives," Translated from *Fizika Goreniya i Vzryva*, Vol. 5, No. 3, 1969, p. 315.

<sup>11</sup> Kuo, K. K., Vichnevetsky, R., and Summerfield, M., "Theory of Flame Front Propagation in Porous Propellant Charges under Confinement," *AIAA Journal*, Vol. 11, No. 4, April 1973, pp. 444-451.

<sup>12</sup> Kuo, K. K., Vichnevetsky, R., and Summerfield, M., "Generation of an Accelerated Flame Front in a Porous Propellant," AIAA Paper 71-210, New York, 1971.

<sup>13</sup> Squire, W. H. and Devine, M. P., "The Interface Between Primer and Propellant," Pt. I and Pt. II, AOA Paper, 1969, Frankford Arsenal, Philadelphia, Pa.

<sup>14</sup> Squire, W. H., private communication, 1970-1971, Frankford Arsenal, Philadelphia, Pa.

<sup>15</sup> Kitchens, C. W., Jr., "Flame Spreading in Small Arms Ball Propellant," Rept. 1604, Aug. 1972, Ballistic Research Labs., Aberdeen Proving Ground, Md.

<sup>16</sup> Kondrikov, B. N. and Ma, C. Y., "The Effect of Pressure and Temperature on the Burning of Powdery Explosive Materials in Low

Density Charges," *The Theory of Explosive Materials*, Moscow, 1967, pp. 207-221.

<sup>17</sup> Bobolev, V. K., Karpukhin, I. A., and Chuiko, S. V., "Combustion of Porous Charges," *Journal of Combustion, Explosion and Shock Waves*, Vol. 1, No. 4, 1966, pp. 31-36.

<sup>18</sup> Bird, R. B., Stewart, W. E., and Lightfoot, E. N., *Transport Phenomena*, Wiley, New York, 1960, pp. 180-200.

<sup>19</sup> Eckert, E. R. G. and Drake, R. M., Jr., *Heat and Mass Transfer*, McGraw-Hill, New York, 1959, pp. 248-253.

<sup>20</sup> Soo, S. L., *Fluid Dynamics of Multiphase Systems*, Blaisdell, Waltham, Mass., 1967, Chap. 6, pp. 248-276.

<sup>21</sup> Williams, F. A., *Combustion Theory*, Addison-Wesley, Reading, Mass., 1965, Chap. 2.

<sup>22</sup> Glazkova, A. P. and Tereshkin, I. A., "Pressure Dependence of the Burning Velocity of Explosives," *Russian Journal of Physical Chemistry*, Vol. 35, No. 7, July 1961, pp. 795-800.

<sup>23</sup> Belyaev, A. F., Korotkov, A. I., Parfenov, A. K., and Sulimov, A. A., "Burning Velocities of Explosives under Very High Pressures," *Russian Journal of Physical Chemistry*, Vol. 37, No. 1, Jan. 1963, pp. 70-74.

JANUARY 1974

AIAA JOURNAL

VOL. 12, NO. 1

## Turbojet Exhaust Reactions in Stratospheric Flight

L. B. ANDERSON\* AND J. W. MEYER†

Lockheed Palo Alto Research Laboratory, Palo Alto, Calif.

AND

W. J. MCLEAN‡

Cornell University, Ithaca, N.Y.

This paper summarizes computational results from chemical modeling of hot turbojet exhaust reactions under high-altitude flight conditions. Interest is in the near-field chemical fate of potential stratospheric pollutants in aircraft wakes. It is found that oxidation and reduction rates of carbon, nitrogen and sulfur species are controlled by super-equilibrium concentrations of radicals. Where there is complete afterburner oxidation of all hydrocarbons, H, O and OH radicals control the nozzle and exhaust jet core reactions. Under these conditions all  $\text{NO}_x$  is present as nitric oxide. However, if high levels of unburned hydrocarbons are present at the exhaust nozzle throat,  $\text{HO}_2$ , OH, and organic molecules are the dominant radical species. In this case there is appreciable production of  $\text{H}_2\text{O}_2$  and  $\text{NO}_2$  in the exhaust. Thus, under certain operating conditions, some  $\text{NO}_x$  may be converted to nitric acid in an aircraft wake. This process is expected to depend on exhaust composition and on cooling and dilution rates in the wake.

### I. Introduction

ENVIRONMENTAL effects of high-altitude aircraft are of mounting interest as the number of flights at stratospheric altitudes increases. Emissions at high altitudes are particularly important because of the relatively long species residence times in the stratosphere. Concern has been expressed over the effect of emissions on the stratospheric ozone layer shielding the Earth

from ultraviolet radiation, and catalytic destruction of ozone by nitrogen oxide ( $\text{NO}_x$ ) emissions may be an important consideration in high-altitude aircraft operations.

For any systematic attempt to evaluate the ultimate environmental impact of exhaust emissions in stratospheric flight, a knowledge of the amounts of potentially important species which are deposited in the stratosphere is needed. Experimental measurements made in the hot exhaust gas near the exit regions of representative aircraft engines may not provide this information for at least two reasons. First, some potentially important species may be inaccessible to quantitative measurement techniques under these conditions. Second, chemical reactions in the exhaust may destroy or give rise to potentially important species downstream from the exit plane of the engine.

The objective of the present study is to determine the nature and extent of those chemical reactions in the near-field flow which can alter the composition of environmentally significant species as the exhaust gases expand and cool to ambient

Presented as Paper 73-99 at the AIAA 11th Aerospace Sciences Meeting, Washington, D.C., January 10-12, 1973; submitted February 23, 1973; revision received August 27, 1973. This work has been supported by the Climatic Impact Assessment Program Office of the Secretary, U.S. Department of Transportation.

Index categories: Reactive Flows; Combustion in Gases; Thermochemistry and Chemical Kinetics.

\* Manager, Chemistry Laboratory, Associate Fellow AIAA.

† Associate Research Scientist, Associate Member AIAA.

‡ Assistant Professor, Sibley School of Mechanical and Aerospace Engineering.

conditions. Any substantial net conversion of photocatalytically active nitrogen oxide to relatively inert nitric acid may be cited as an example of the type of reaction which would be considered potentially significant if it occurred in the exhaust regime. Computation of the  $\text{NO}/\text{NO}_2$  ratio as a function of distance behind the aircraft represents an unnecessary task for this objective if substantial  $\text{NO}_x$  conversion to  $\text{HNO}_3$  does not take place, however. The reason is that after dilution, when ozone concentrations are higher than  $\text{NO}_x$  concentrations, reactions in the stratosphere will adjust  $\text{NO}/\text{NO}_2$  ratios quite rapidly (within minutes) to the appropriate local steady-state values before there is a significant environmental impact. Here, the total  $\text{NO}_x$  added is the important variable, not the detailed history of the  $\text{NO}$  and  $\text{NO}_2$  concentrations in the aircraft wake.

To satisfy the stated objective, three questions have been considered. First, what kind of chemistry characterizes the exhaust jet region? Is it strongly nonequilibrium, are atom and radical reactions important, and so forth? Second, is it possible to discover simplifying interrelationships among reactions and species so that, from knowledge of some of the variables (e.g., from engine test data), the evolving exhaust composition can then be adequately predicted for a variety of conditions? And third, what is the sensitivity of predicted emission concentrations to uncertainties in the data employed, such as measured concentrations or rate constants?

Although not addressed explicitly, these questions are answered in the sections which follow. The section on development and execution of model calculations gives results which clearly define the nature of the relevant exhaust chemistry. The sections which analyze the governing relationships among  $\text{CO}_x$ ,  $\text{NO}_x$ ,  $\text{SO}_x$ , and hydrocarbons succeed in simplifying the chemistry and the data requirements for predictive purposes. Finally, the brief discussion of the chemical system sensitivity to changes in selected rate constants deals with the last of the preceding questions.

For the studies of thermal reactions in the engine exhaust regime, the analytical approach involves setting up a chemical kinetics model using those elementary reactions which play a role in changing the concentrations of engine emissions in the exhaust nozzle and the near-jet downstream from the engine exit plane. Numerical methods are used to integrate the resultant governing chemical rate equations up to the point where the exhaust flow mixes with the ambient atmosphere. Initial conditions for the computation are compatible with available data on engine exhaust composition.

A model consisting of elementary forward and backward reactions has been used in this study. Reaction rate constants are taken from recent evaluations available in the literature. The fluid dynamic structure of the exhaust jet region is also taken from theoretical and experimental data available from the literature.

## II. Description of Models

### Fluid Mechanics

The sample results presented here are for an engine equipped with a secondary nozzle designed to obtain an ideal pressure-matched condition at the nozzle exit plane. After leaving the nozzle, the exhaust flow forms a turbulent jet, as shown by Fig. 1. The boundaries of this jet are free turbulent shear layers between the jet core and the supersonic freestream. These shear layers grow as the jet proceeds downstream until they meet at the center, after which the exhaust becomes a fully developed turbulent jet. In the region between this meeting point and the exit plane of the exhaust nozzle there exists in the center of the jet a conical region which is unaffected by the external stream; with the nozzle expansion matched to ambient pressure, the flow properties are constant in this region. Hence, the exhaust gas temperature on the jet centerline will be constant, equal to its value at the nozzle exit, downstream to the point where the shear layers meet. For conservative analysis, it is necessary to determine the longest possible initial constant temperature core.

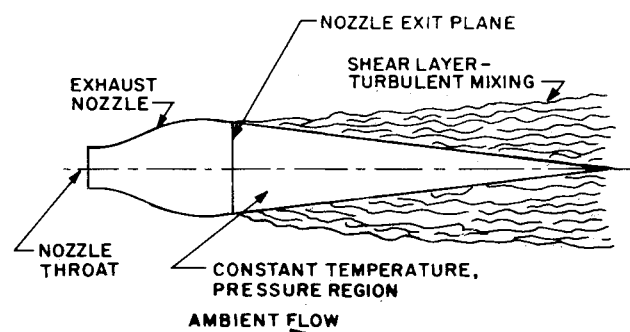


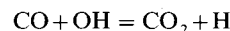
Fig. 1 Idealization of near-jet exhaust.

From the theory of Abramovich<sup>1</sup> for a condition of full-power operation of the GE-4 engine at 65,000 ft, and an aircraft Mach number of 2.7, the length of the initial core region of constant temperature is found to be 22.15 m. Experiments pertaining to this situation were carried out by Forstall and Shapiro,<sup>2</sup> and an expression was derived for the length of this core by curve-fitting data. Use of this expression yields a value of 22.0 m for the length of the constant-temperature core.

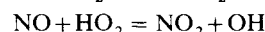
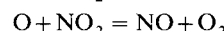
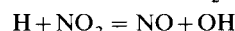
The complete chemical kinetic model analysis along the center streamline then involves two steps. First, the model is run subject to the constraint of the expansion nozzle flow. Second, the calculations are continued at the exit-plane temperature and pressure out to the end of the unmixed region.

### Chemical Kinetics

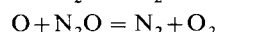
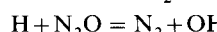
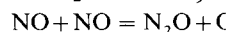
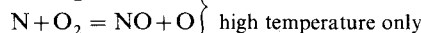
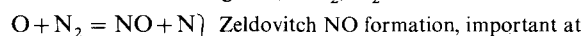
The only significant carbon monoxide oxidation step is



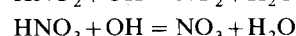
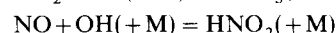
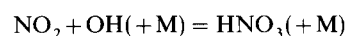
The reactions  $\text{CO} + \text{O} + \text{M} \rightarrow \text{CO}_2 + \text{M}$  or  $\text{CO} + \text{O}_2 \rightarrow \text{CO}_2 + \text{O}$  are negligibly slow. Principal reactions exchanging  $\text{NO}$  and  $\text{NO}_2$  are



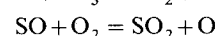
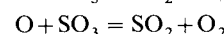
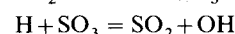
Other reactions involving  $\text{NO}$ ,  $\text{NO}_2$ ,  $\text{N}_2\text{O}$  are



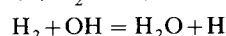
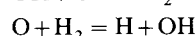
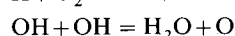
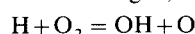
The nitric and nitrous acid reactions are



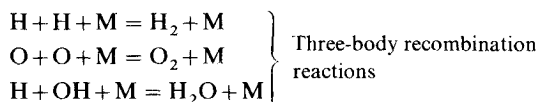
Sulfur reactions are



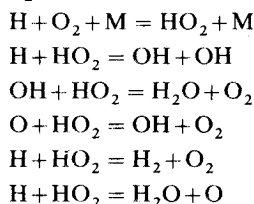
Reactions affecting  $\text{H}$ ,  $\text{O}$ , and  $\text{OH}$  radical concentrations are



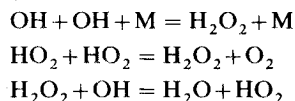
Fast bimolecular radical  
shuffle reactions



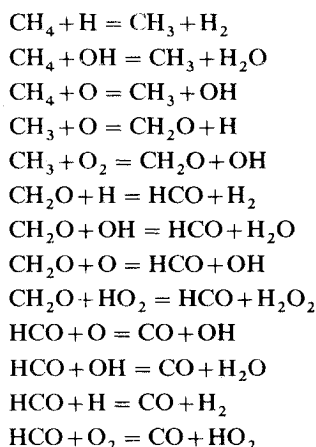
Reactions of the  $\text{HO}_2$  radical are



Reactions of  $\text{H}_2\text{O}_2$  are



The preceding 72 reactions (forward and reverse) can be taken to describe the fuel-lean chemistry in the engine exhaust nozzle and plume up to the point where mixing between the exhaust plume and the surrounding atmosphere becomes important. A necessary condition for their sufficiency is that the hydrocarbon emissions be very low so that carbon monoxide oxidation is dominant. For local conditions where this is not the case, the following methane oxidation scheme is used to represent HC oxidation:



The analyses of the effect of the chemical reactions in the engine nozzle and exhaust plume were carried out using the NASA Lewis general chemical kinetics computer program.<sup>3</sup> The NASA program is capable of treating chemical reactions coupled with the fluid mechanical equations of one-dimensional flow.

Rate constant data used in the model are listed in Table 1. The Arrhenius parameters given there refer to the forward direction of the reaction as written; respective reverse rates are computed from thermodynamic information.

Various conceivable reactions do not appear in Table 1 when previous computations have shown them to be unimportant (e.g.,  $\text{N} + \text{N} + \text{M} \rightarrow \text{N}_2 + \text{M}$ ), or when they have been evaluated as not important (e.g.,  $\text{HNO}_2 + \text{O} + \text{M} \rightarrow \text{HNO}_3 + \text{M}$ ) (Ref. 24). In some cases, reactions which are thought to occur but for which data are lacking have been assumed to be similar to other reactions which have been studied. For example, the rate constant for the reaction (54)  $\text{HNO}_2 + \text{OH} \rightarrow \text{NO}_2 + \text{H}_2\text{O}$  was estimated<sup>22</sup> as being identical to the following: (53)  $\text{HNO}_3 + \text{OH} \rightarrow \text{NO}_3 + \text{H}_2\text{O}$ . The evaluator states that the expected error of this estimate is at least a factor of three.<sup>22</sup>

In the methane oxidation scheme the important reaction (46) has an estimated rate constant with an unspecified error.<sup>19</sup> Based on an earlier private communication, the rate constant shown in Table 1 for the reaction (6)  $\text{NO} + \text{HO}_2 \rightarrow \text{NO}_2 + \text{OH}$  is about a factor of four higher than a more recent recommendation.<sup>24</sup>

As stated, fluid mechanical constraints for the present calculations were chosen to reflect a Mach 2.7 flight with the GE-4

Table 1 Chemical reactions in the  $\text{CO}_x/\text{NO}_x/\text{SO}_x/\text{CH}_4/\text{air}$  system

Reaction	Reaction rate variables <sup>a</sup>				Ref
	A	n	E		
1 $\text{H} + \text{N}_2\text{O} = \text{N}_2 + \text{OH}$	$3.0 \times 10^{13}$	0	40.8		4
2 $\text{N} + \text{OH} = \text{NO} + \text{H}$	$4.2 \times 10^{13}$	0	0		4
3 $\text{O} + \text{N}_2\text{O} = \text{N}_2 + \text{O}_2$	$3.6 \times 10^{13}$	0	24.0		5
4 $\text{N}_2 + \text{NO}_2 = \text{NO} + \text{N}_2\text{O}$	$1.4 \times 10^{14}$	0	83.0		5
5 $\text{H} + \text{NO}_2 = \text{NO} + \text{OH}$	$7.25 \times 10^{14}$	0	1.93		6
6 $\text{HO}_2 + \text{NO} = \text{OH} + \text{NO}_2$	$6.0 \times 10^{11}$	0	0		7
7 $\text{O} + \text{N}_2 = \text{NO} + \text{N}$	$5.0 \times 10^{13}$	0	75.0		8
8 $\text{NO} + \text{O} = \text{N} + \text{O}_2$	$3.1 \times 10^9$	1	39.1		8
9 $\text{NO} + \text{O} + \text{M} = \text{NO}_2 + \text{M}$	$1.05 \times 10^{15}$	0	-1.87		9
10 $\text{NO}_2 + \text{O} = \text{NO} + \text{O}_2$	$1.0 \times 10^{13}$	0	0.6		9
11 $\text{NO} + \text{NO} = \text{N}_2\text{O} + \text{O}$	$7.05 \times 10^{11}$	0	65.0		10
12 $\text{M} + \text{N}_2\text{O} = \text{N}_2 + \text{O} + \text{M}$	$6.3 \times 10^{14}$	0	56.8		8
13 $\text{CO} + \text{OH} = \text{CO}_2 + \text{H}$	$3.1 \times 10^{11}$	0	0.6		11
14 $\text{H} + \text{O}_2 = \text{OH} + \text{O}$	$2.2 \times 10^{14}$	0	16.8		12
15 $\text{OH} + \text{OH} = \text{H}_2\text{O} + \text{O}$	$6.3 \times 10^{12}$	0	1.1		12
16 $\text{O} + \text{H}_2 = \text{H} + \text{OH}$	$1.8 \times 10^{10}$	1	8.9		12
17 $\text{H}_2 + \text{OH} = \text{H}_2\text{O} + \text{H}$	$2.2 \times 10^{13}$	0	5.15		12
18 $\text{H} + \text{H} + \text{M} = \text{H}_2 + \text{M}$	$3.0 \times 10^{15}$	0	0		12
19 $\text{M} + \text{H} + \text{OH} = \text{H}_2\text{O} + \text{M}$	$1.4 \times 10^{23}$	-2	0		12
20 $\text{O} + \text{O} + \text{M} = \text{O}_2 + \text{M}$	$2.6 \times 10^{17}$	-0.93	0		8
21 $\text{M} + \text{H} + \text{O}_2 = \text{HO}_2 + \text{M}$	$1.5 \times 10^{15}$	0	-1.0		12
22 $\text{H} + \text{HO}_2 = \text{OH} + \text{OH}$	$2.5 \times 10^{14}$	0	1.9		12
23 $\text{OH} + \text{HO}_2 = \text{H}_2\text{O} + \text{O}_2$	$1.0 \times 10^{13}$	0	1.0		13
24 $\text{O} + \text{HO}_2 = \text{OH} + \text{O}_2$	$5.0 \times 10^{13}$	0	1.0		12
25 $\text{H} + \text{HO}_2 = \text{H}_2 + \text{O}_2$	$2.5 \times 10^{13}$	0	0.7		12
26 $\text{H} + \text{HO}_2 = \text{H}_2\text{O} + \text{O}$	$1.0 \times 10^{13}$	0	1.0		12
27 $\text{NO}_2 + \text{OH} = \text{HNO}_3$	$1.2 \times 10^{12}$	0	0		14
28 $\text{H}_2\text{O}_2 + \text{OH} = \text{H}_2\text{O} + \text{HO}_2$	$1.0 \times 10^{13}$	0	1.8		12
29 $\text{OH} + \text{OH} + \text{M} = \text{H}_2\text{O}_2 + \text{M}$	$7.1 \times 10^{14}$	0	-5.1		12
30 $\text{HO}_2 + \text{HO}_2 = \text{H}_2\text{O}_2 + \text{O}_2$	$2.0 \times 10^{12}$	0	0		12
31 $\text{SO}_2 + \text{O} + \text{M} = \text{SO}_3 + \text{M}$	$4.5 \times 10^{14}$	0	0		15
32 $\text{SO}_3 + \text{H} = \text{SO}_2 + \text{OH}$	$6.5 \times 10^{14}$	0	10.8		15
33 $\text{SO}_3 + \text{O} = \text{SO}_2 + \text{O}$	$6.5 \times 10^{14}$	0	10.8		15
34 $\text{CH}_4 + \text{H} = \text{CH}_3 + \text{H}_2$	$4.0 \times 10^{14}$	0	11.6		16
35 $\text{CH}_4 + \text{OH} = \text{CH}_3 + \text{H}_2\text{O}$	$2.9 \times 10^{13}$	0	5.0		11
36 $\text{CH}_4 + \text{O} = \text{CH}_3 + \text{OH}$	$2.1 \times 10^{13}$	0	9.1		17
37 $\text{CH}_3 + \text{O} = \text{CH}_2\text{O} + \text{H}$	$1.9 \times 10^{13}$	0	0		16
38 $\text{CH}_3 + \text{O}_2 = \text{CH}_2\text{O} + \text{OH}$	$1.0 \times 10^{10}$	0	0		18
39 $\text{CH}_2\text{O} + \text{HO}_2 = \text{HCO} + \text{H}_2\text{O}_2$	$4.8 \times 10^{12}$	0	6.6		13
40 $\text{CH}_2\text{O} + \text{H} = \text{HCO} + \text{H}_2$	$1.0 \times 10^{13}$	0	2.0		16
41 $\text{CH}_2\text{O} + \text{OH} = \text{HCO} + \text{H}_2\text{O}$	$5.1 \times 10^{15}$	0	13.0		11
42 $\text{CH}_2\text{O} + \text{O} = \text{HCO} + \text{OH}$	$4.8 \times 10^{12}$	0	6.6		19
43 $\text{HCO} + \text{O} = \text{CO} + \text{OH}$	$1.8 \times 10^{11}$	0.5	0		16
44 $\text{HCO} + \text{OH} = \text{CO} + \text{H}_2\text{O}$	$1.1 \times 10^{11}$	0.5	0		16
45 $\text{HCO} + \text{H} = \text{CO} + \text{H}_2$	$1.5 \times 10^{12}$	0.5	0		16
46 $\text{HCO} + \text{O}_2 = \text{CO} + \text{HO}_2$	$1.0 \times 10^{11}$	0	0		19
47 $\text{O} + \text{O}_2 + \text{M} = \text{O}_3 + \text{M}$	$1.7 \times 10^{13}$	0	-2.1		20
48 $\text{O} + \text{O}_3 = \text{O}_2 + \text{O}_2$	$1.2 \times 10^{13}$	0	4.8		20
49 $\text{H} + \text{O}_3 = \text{OH} + \text{O}_2$	$1.6 \times 10^{13}$	0	0		21
50 $\text{NO} + \text{O}_3 = \text{NO}_2 + \text{O}_2$	$6.7 \times 10^{11}$	0	2.45		21
51 $\text{OH} + \text{H}_2\text{O}_2 = \text{H}_2 + \text{HO}_2$	$1.0 \times 10^{13}$	0	1.8		12
52 $\text{NO} + \text{OH} + \text{M} = \text{HNO}_2 + \text{M}$	$2.4 \times 10^{16}$	0	-1.6		14
53 $\text{HNO}_3 + \text{OH} = \text{NO}_3 + \text{H}_2\text{O}$	$8.4 \times 10^{11}$	0	2.0		22
54 $\text{HNO}_2 + \text{OH} = \text{NO}_2 + \text{H}_2\text{O}$	$8.4 \times 10^{11}$	0	2.0		22
55 $\text{SO} + \text{O}_2 = \text{SO}_2 + \text{O}$	$1.8 \times 10^{11}$	0	5.6		23

<sup>a</sup> Reaction rate constant  $k = AT^n \exp(-E/RT)$ . Units are moles, cm, sec, °K, Kcal.

engine at a power setting of 1 (maximum power), and at a 65,000-ft altitude. The exhaust jet temperature was 945°K, which was maintained on the exhaust centerline out to a distance of 22 m—the end of the core of constant properties in this case. In a sense, these conditions constitute a representative upper limit for reactions most likely to affect pollutant species, primarily because exhaust temperatures are higher with afterburning.

The initial composition for the nozzle expansion was taken to be that determined by chemical equilibrium at the nozzle throat, with the exception of  $\text{CO}$ ,  $\text{NO}$  and  $\text{NO}_2$  (equilibrium calculations were performed using a Lockheed Thermochemical equilibrium program). The species  $\text{CO}$  and  $\text{NO}$  are well known

Table 2 Initial throat concentrations<sup>a</sup>

Species	Mole fraction
H	7.57 E-07
N <sub>2</sub> O	8.11 E-08
N <sub>2</sub>	7.47 E-01
OH	3.33 E-04
NO	3.00 E-04
O	1.56 E-05
O <sub>2</sub>	5.59 E-02
NO <sub>2</sub>	3.00 E-05
HO <sub>2</sub>	1.36 E-07
CO	3.00 E-03
CO <sub>2</sub>	9.10 E-02
H <sub>2</sub> O	1.02 E-01
H <sub>2</sub>	1.28 E-05
HNO <sub>3</sub>	1.00 E-11
HNO <sub>2</sub>	1.00 E-09
SO	1.00 E-08
SO <sub>2</sub>	5.00 E-05
SO <sub>3</sub>	1.00 E-08

<sup>a</sup> Static temperature, 1730°K; static pressure, 0.893 atm; equivalent fuel, C<sub>8</sub>H<sub>18</sub>; equivalence ratio, 0.715.

to be out of equilibrium in jet exhaust because of chemical kinetic freezing effects in the combustor region. CO and NO concentrations have been estimated by a review of available aircraft exhaust emission data. NO<sub>2</sub> concentration has been arbitrarily given a large value—10% of the NO concentration—for the purpose of illustrating the difficulty of preserving NO<sub>2</sub>. Actual NO<sub>2</sub> levels in jet exhausts are highly uncertain at present.

Initial throat concentrations of all species considered in the

first runs are given in Table 2. Hydrocarbons and H<sub>2</sub>O<sub>2</sub> were not taken into consideration for this particular case. Under these starting conditions, the model calculations yielded the concentration profiles shown in Fig. 2. Excluded from Fig. 2 are some trace species like HNO<sub>3</sub> and N, whose concentration levels remain at all times less than 1 ppb, and the major species CO<sub>2</sub>, O<sub>2</sub>, N<sub>2</sub>, and H<sub>2</sub>O. Concentrations calculated from thermodynamic equilibrium considerations are indicated on the far right of the figure for comparison.

#### Discussion of Kinetics without Excess Hydrocarbons

The results in Fig. 2 show that a nonequilibrium, but only slowly changing, chemical balance exists in the exhaust plume. Evidently, at the low density corresponding to 65,000-ft altitude, recombination is very slow. All of the active inorganic radical and atomic species are found to exist in superequilibrium concentrations.

The origin and maintenance of these radicals is a consequence of carbon monoxide oxidation. At throat temperature, CO + OH → CO<sub>2</sub> + H is essentially a branching step because the H atoms produced react via H + O<sub>2</sub> → O + OH, followed by O + H<sub>2</sub>O → OH + OH and H + H<sub>2</sub>O → H<sub>2</sub> + OH.

In the cooler exhaust jet, CO oxidation is still a chain mechanism since now CO + OH → CO<sub>2</sub> + H is followed mainly by H + O<sub>2</sub> + M → HO<sub>2</sub> + M and then H + HO<sub>2</sub> → OH + OH. This notion that the high radical concentrations are a result of carbon monoxide oxidation as the driving reaction is confirmed by computations in which the CO oxidation rate is arbitrarily reduced to negligible values. The output then shows an order of magnitude lower in concentrations of O, H, and OH radicals in the nozzle.

Understanding the details of the various chemical balances is aided by Table 3. There are listed rate constants, forward reaction rates, and net rates for the various reactions at a position

Table 3 Chemical kinetic situation 2.7-m downstream of nozzle exit plane

Reaction	Forward reaction rate (mole/cm <sup>3</sup> -sec)	Net reaction rate (mole/cm <sup>3</sup> -sec)	Comments <sup>a</sup>
1 H + N <sub>2</sub> O = N <sub>2</sub> + OH	9.24 E-13	9.24 E-13	F
3 O + N <sub>2</sub> O = N <sub>2</sub> + O <sub>2</sub>	8.45 E-16	8.45 E-16	F
4 N <sub>2</sub> + NO <sub>2</sub> = NO + N <sub>2</sub> O	1.56 E-26	-5.11 E-21	R
5 H + NO <sub>2</sub> = NO + OH	1.66 E-10	1.66 E-10	F
6 HO <sub>2</sub> + NO = OH + NO <sub>2</sub>	1.38 E-11	1.38 E-11	F
9 NO <sub>2</sub> + M = NO + O + M	2.92 E-20	-1.31 E-10	R
10 NO <sub>2</sub> + O = O <sub>2</sub> + NO	4.08 E-12	4.08 E-12	F
11 NO + NO = N <sub>2</sub> O + O	3.21 E-23	-1.14 E-16	R
12 N <sub>2</sub> O + M = N <sub>2</sub> + O + M	1.68 E-18	-2.79 E-14	R
13 CO + OH = CO <sub>2</sub> + H	3.34 E-8	3.17 E-8	B
14 H + O <sub>2</sub> = OH + O	1.90 E-7	5.16 E-9	Fastest reaction but very near PE
15 OH + OH = H <sub>2</sub> O + O	3.44 E-8	-3.43 E-9	Near PE
16 O + H <sub>2</sub> = H + OH	3.21 E-9	-1.52 E-10	Near PE
17 H <sub>2</sub> + OH = H <sub>2</sub> O + H	2.01 E-8	-3.05 E-9	Near PE
18 H <sub>2</sub> + M = H + H + M	1.22 E-24	-1.01 E-10	R
19 H + OH + M = H <sub>2</sub> O + M	1.90 E-9	1.90 E-9	F
20 O <sub>2</sub> + M = O + O + M	2.44 E-26	-1.87 E-12	R
21 M + H + O <sub>2</sub> = HO <sub>2</sub> + M	1.23 E-8	1.23 E-8	F
22 H + HO <sub>2</sub> = OH + OH	7.77 E-9	7.77 E-9	F
23 OH + HO <sub>2</sub> = H <sub>2</sub> O + O <sub>2</sub>	3.46 E-10	3.46 E-10	F
24 O + HO <sub>2</sub> = OH + O <sub>2</sub>	2.21 E-9	2.21 E-9	F
25 H + HO <sub>2</sub> = H <sub>2</sub> + O <sub>2</sub>	1.48 E-9	1.48 E-9	F
26 H + HO <sub>2</sub> = H <sub>2</sub> O + O	5.03 E-10	5.03 E-10	F
27 NO <sub>2</sub> + OH = HNO <sub>3</sub>	4.40 E-12	6.75 E-17	PE
31 SO <sub>2</sub> + O + M = SO <sub>3</sub> + M	1.36 E-12	1.36 E-12	F
32 SO <sub>3</sub> + H = SO <sub>2</sub> + OH	7.32 E-13	7.32 E-12	F
33 SO <sub>3</sub> + O = SO <sub>2</sub> + O <sub>2</sub>	6.42 E-13	6.42 E-13	F
52 NO + OH + M = HNO <sub>2</sub> + M	8.80 E-10	1.25 E-10	B
54 HNO <sub>2</sub> + OH = NO <sub>2</sub> + H <sub>2</sub> O	2.55 E-11	2.55 E-11	F
55 SO + O <sub>2</sub> = SO <sub>2</sub> + O	1.01 E-12	5.92 E-13	B

<sup>a</sup> F forward reaction dominates. R reverse reaction dominates. PE forward rate = reverse rate, reaction in partial equilibrium. B both forward and back rates significant and nonequal.

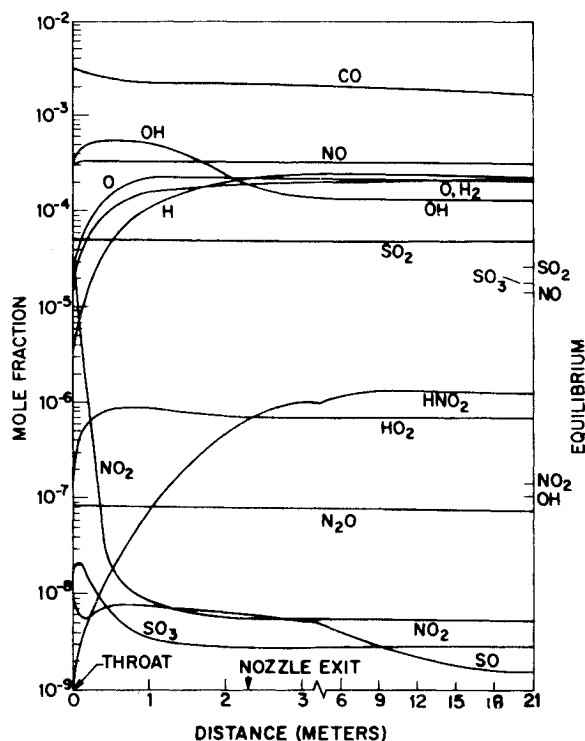


Fig. 2 Centerline concentration profiles, GE-4 secondary nozzle and exhaust (zero  $\text{CH}_4$  at throat).

2 m downstream from the nozzle exit plane. Table 3 can then in turn be used to identify the reactions which are of importance to individual species rates. For example, the OH balance shown in Table 4 is instructive. This gives all the important reactions involving OH as well as their rates and the net effect. As can be seen in the table, the aforementioned CO oxidation chain has the consequence that the net disappearance of OH is more than an order of magnitude less than its rate of participation in  $\text{CO} + \text{OH} \rightarrow \text{CO}_2 + \text{H}$ . Hence, it would be a good approximation to assume the OH concentration constant in computing the rate of CO oxidation. It is encouraging to note that a recent optical measurement<sup>25,26</sup> of OH concentration in a relevant afterburning situation under altitude condition gives an OH concentration in good agreement with the superequilibrium value computed here.

#### Exhaust Chemistry with Significant Hydrocarbons

Test data are somewhat scarce for SST engines, but existing data show that quantities of unburned hydrocarbons (measured as total C) may be large along certain streamlines with afterburning.<sup>26</sup> To take some account of the effect of hydrocarbons on the chemistry, reactions (34–46), a methane oxidation scheme, have been included at this point. Admittedly, the oxidation schemes for other hydrocarbons are different from that of methane. Radical scavenging and termination reactions involving larger organic molecules can be very rapid. Numerous other differences exist. However, the fractions and identity of unburned fuel molecular fragments in hot jet exhausts are unknown at present, and results are typically given as total ppm-C or as equivalent  $\text{CH}_4$ . Some methane has been observed in jet exhausts.<sup>26</sup> If significant  $\text{NO}_2$  can be formed as a consequence of unburned methane oxidation, the higher hydrocarbons are likely to produce a similar effect. This is because the formation of methyl radicals is a sufficient starting condition for the subsequent oxidation steps leading to  $\text{NO}_2$ . During combustion, there is a strong tendency for the higher HC's to form alkyl radicals or olefins which then form the alkyl radicals by addition reactions. The alkyl radicals can decompose to give methyl radicals and the next lower olefin.<sup>27</sup> The presence of methyl

radicals in the hot oxidizing atmosphere leads to production of formyl radicals. Then, key reactions leading to induced  $\text{NO}_2$  formation are the abstraction by molecular oxygen of reactive hydrogen from formyl radicals, with accompanying reductions in the concentrations of H and O atoms which would otherwise destroy the  $\text{NO}_2$ .

Two sets of concentration profiles are shown in Figs. 3 and 4. Both are for the same operating condition as Fig. 1. Starting throat concentrations of all species are taken as before, except that the portion of  $\text{CH}_4$  is assumed initially at 500 ppm in Fig. 3 and 3000 ppm in Fig. 4. In the first case, most of the  $\text{CH}_4$  is oxidized in the nozzle and jet, with about a five-fold reduction in total HC (including  $\text{CH}_2\text{O}$ ,  $\text{CH}_3$ , and  $\text{HCO}$ ) by the time the nozzle exit plane is reached, with further reductions to about 5 ppm total HC at the jet tip where mixing with ambient air begins. The concentrations of H, O, and OH are still quite large near the tip of the isothermal core region.

When the  $\text{CH}_4$  is set at 3000 ppm throat concentration, only about two thirds of the methane is completely oxidized before mixing with ambient air begins along the axial streamline. In this case H and O are greatly reduced while large amounts of  $\text{CH}_2\text{O}$  and  $\text{HO}_2$  appear. The most significant result in this case is the rapid conversion of nitric oxide to  $\text{NO}_2$  in the exhaust. At the apex of the core region, Fig. 4 shows that the  $\text{NO}_2$  has increased to one third of the NO concentration. This result is in general agreement with experimental observations that the appearance of  $\text{NO}_2$  is associated with afterburning. Such observations have been made in tests of Olympus 593 engine, for example.<sup>28</sup> In recent emission tests of a J85-GE-13 turbojet a direct correlation of  $\text{NO}_2$  fraction of total  $\text{NO}_x$  with hydrocarbon concentration is quite evident.<sup>29</sup>

An examination of the chemistry leading to  $\text{NO}_2$  production

Table 4 Predominant contributions to OH balance 2.7-m downstream of exhaust nozzle exit plane

Reaction			Comment
OH formations			
22	$\text{H} + \text{HO}_2$	$\rightarrow \text{OH} + \text{OH}$	Primary
15	$\text{H}_2\text{O} + \text{O}$	$\rightarrow \text{OH} + \text{OH}$	
14	$\text{H} + \text{O}_2$	$\rightarrow \text{OH} + \text{O}$	Secondary
17	$\text{H}_2\text{O} + \text{H}$	$\rightarrow \text{H}_2 + \text{OH}$	
24	$\text{O} + \text{HO}_2$	$\rightarrow \text{OH} + \text{O}_2$	
OH destructions			
13	$\text{CO} + \text{OH}$	$\rightarrow \text{CO}_2 + \text{H}$	Primary
19	$\text{H} + \text{OH} + \text{M}$	$\rightarrow \text{H}_2\text{O} + \text{M}$	Secondary
23	$\text{OH} + \text{HO}_2$	$\rightarrow \text{H}_2\text{O} + \text{O}_2$	Small contributions
5	$\text{H} + \text{NO}_2$	$\rightarrow \text{NO} + \text{OH}$	
16	$\text{H} + \text{OH}$	$\rightarrow \text{O} + \text{H}_2$	
52	$\text{NO} + \text{OH} + \text{M}$	$\rightarrow \text{HNO}_2 + \text{M}$	
Net change OH		Contribution to $\left(\frac{\text{moles}}{\text{cm}^3\text{-sec}}\right)$	
Reaction			
22		1.56 E-8	
15		0.86 E-8	
14		0.58 E-8	
17		0.31 E-8	
24		0.22 E-8	
13		-3.17 E-8	
19		-0.19 E-8	
23		-0.03 E-8	
5		-0.02 E-8	
16		-0.02 E-8	
52		-0.01 E-8	
Net $\frac{d(\text{OH})}{dt} =$		-0.12 E-8 $\left(\frac{\text{moles}}{\text{cm}^3\text{-sec}}\right)$	
To be compared with $\frac{d(\text{CO})}{dt} =$		-3.17 E-8 $\left(\frac{\text{moles}}{\text{cm}^3\text{-sec}}\right)$	

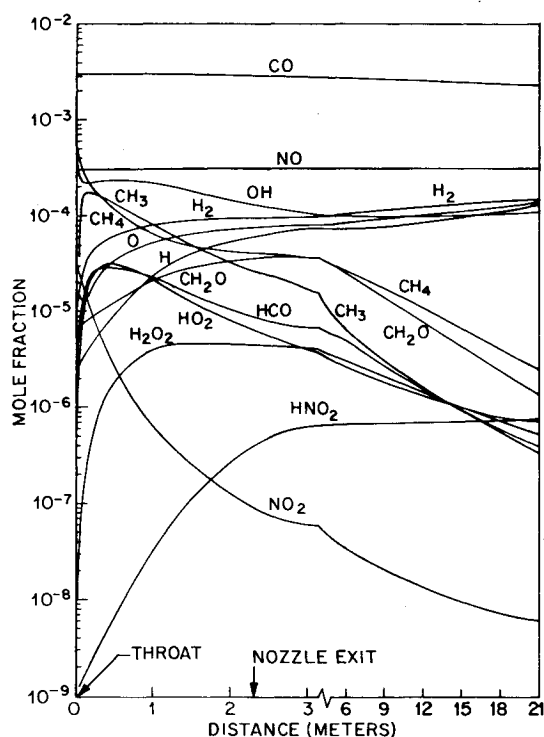
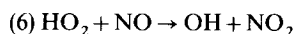


Fig. 3 Centerline concentration profiles, GE-4 secondary nozzle and exhaust (500 ppm  $\text{CH}_4$  at throat).

is instructive. The high concentrations of  $\text{HO}_2$  which oxidize NO, i.e.,



would not be possible without the rapid production of HCO in the hydrocarbon oxidation process, because it is HCO rather than H which leads to a high net yield of  $\text{HO}_2$

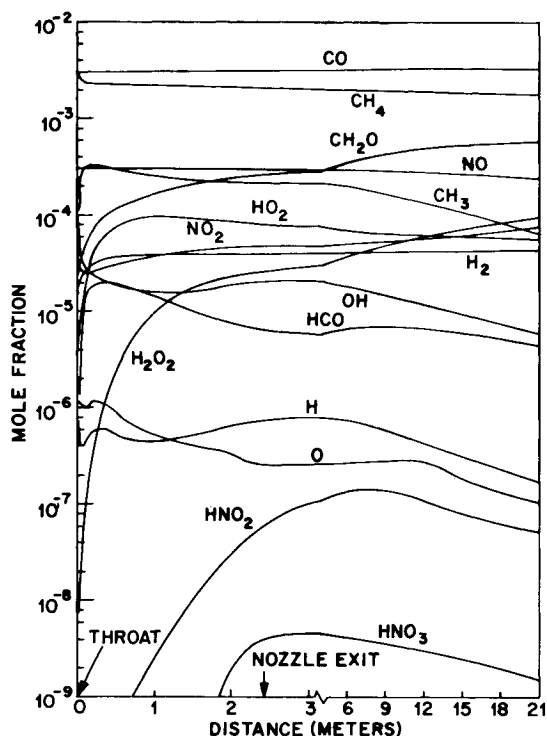
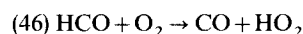
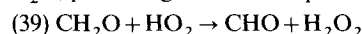


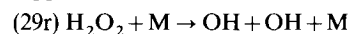
Fig. 4 Centerline concentration profiles, GE-4 secondary nozzle and exhaust (3000 ppm  $\text{CH}_4$  at throat).



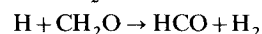
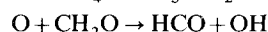
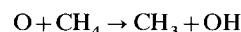
From examination of the reaction rates in the computer output at the 5-m position in Fig. 4 (2.7-m downstream from the nozzle exit) the following insight is gained. Much, but not all, of the  $\text{HO}_2$  made primarily by reaction (46) is converted to hydrogen peroxide by  $\text{CH}_2\text{O}$ , producing CHO in the process



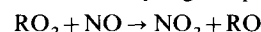
Thermal decomposition of  $\text{H}_2\text{O}_2$  tends to keep OH at reasonably high levels ( $\sim 10$  ppm)



The H and O atom concentrations are low because these are consumed by abstraction reactions with the hydrocarbon species, e.g.,



Thus, the efficient destruction by H and O of  $\text{HO}_2$  and  $\text{NO}_2$  is suppressed and their production is promoted as a consequence of the hydrocarbon oxidation process, without the necessity of involving direct NO oxidation by organic peroxy radicals, i.e.,



Thus, a key role is indicated for the HCO radical in explaining the experimentally observed downstream formation of  $\text{NO}_2$  associated with afterburning. Also, it appears that significant amounts of  $\text{H}_2\text{O}_2$  should form in the exhaust jet core with afterburning when conditions are right for substantial  $\text{NO}_2$  formation.

### III. Governing Relationships

#### Radical Partial Equilibrium

When no excess unburned fuel is present, several simplifying relationships may be deduced. One condition which is evident from Table 3 is that the bimolecular shuffle reactions (14–17) are in partial equilibrium. That is, their forward reaction rates are approximately equal to their reverse rates. This condition is exhibited in the table by the fact that the forward rate is much larger than the net rate. Since the ratio of forward/back rate constant is the equilibrium constant, an algebraic equation can be written relating the concentration of species in each of these reactions, as follows:

$$K_{14} = \frac{[\text{OH}][\text{O}]}{[\text{H}][\text{O}_2]}; \quad K_{15} = \frac{[\text{H}_2\text{O}][\text{O}]}{[\text{OH}]^2}$$

$$K_{16} = \frac{[\text{H}][\text{OH}]}{[\text{O}][\text{H}_2]}; \quad K_{17} = \frac{[\text{H}_2\text{O}][\text{H}]}{[\text{H}_2][\text{OH}]} = K_{15} K_{16}$$

where K represents the equilibrium constants and the brackets signify concentrations. Since only three of these equations are independent, a complete solution is not obtainable, but the concentration of the variable species H, OH,  $\text{H}_2$ , and O can be expressed as a function of just one. If OH is selected as the independent quantity, one has

$$[\text{H}] = \frac{K_{15}}{K_{14}[\text{O}_2][\text{H}_2\text{O}]} [\text{OH}]^3$$

$$[\text{O}] = \frac{K_{15}}{[\text{H}_2\text{O}]} [\text{OH}]^2$$

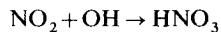
$$[\text{H}_2] = \frac{1}{K_{14}K_{16}[\text{O}_2]} [\text{OH}]^2$$

These relationships are expected to be of value in setting initial conditions for downstream calculations from test cell measurements of OH concentrations.

#### Oxides of Nitrogen

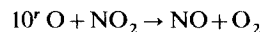
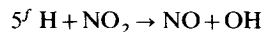
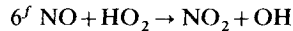
Oxides of nitrogen are the species of major interest with

regard to environmental impact. The portion of  $\text{NO}_x$  as  $\text{NO}_2$  in the hot exhaust is of importance because of the possibility of nitric acid formation to provide an  $\text{NO}_x$  "sink" in the wake



Thermodynamic equilibrium considerations give an  $\text{NO}_2/\text{NO}$  ratio of 0.01 at exit plane conditions. The results of the kinetic calculations without HC, as shown in Fig. 2, reveal that conversion of NO to  $\text{NO}_2$  actually does not occur. In fact, any  $\text{NO}_2$  assumed present at the throat is quickly destroyed. At the exit plane the concentration has fallen to 5 ppb, corresponding to an  $\text{NO}_2/\text{NO}$  ratio of only  $10^{-5}$ .

The  $\text{NO}_2$  is kept below its equilibrium level by fast reactions such as



and the fact that the H and the O levels are maintained far above their equilibrium concentrations. The second and fifth reactions above become unimportant as the temperature drops and are already much slower than the other three reactions at the exit plane.

The contributions to the  $\text{NO}_2$  balance at the 5-m position can be tabulated as follows:

Net Change  $\text{NO}_2$ , No Excess HC

$$r_{9^r} = 1.31 \times 10^{-10} \text{ (Moles/cm}^3\text{-sec)}$$

$$r_{6^f} = 0.14 \times 10^{-10} \text{ (Moles/cm}^3\text{-sec)}$$

$$r_{54^r} = 0.25 \times 10^{-10} \text{ (Moles/cm}^3\text{-sec)}$$

$$-r_{5^f} = 1.66 \times 10^{-10} \text{ (Moles/cm}^3\text{-sec)}$$

$$-r_{10^r} = 0.04 \times 10^{-10} \text{ (Moles/cm}^3\text{-sec)}$$

$$\frac{d[\text{NO}_2]}{dt} = \sum r < 0.01 \times 10^{-10} \text{ (Moles/cm}^3\text{-sec)}$$

Thus, in the absence of HC the  $\text{NO}_2$  level is largely controlled by a steady state between its formation by reaction with O atoms and destruction by H atoms. Given such a balance between reactions (9) and (5), an expression for the steady-state  $\text{NO}_2/\text{NO}$  ratio is obtained as follows:

$$0 = d[\text{NO}_2]/dt = k_9[\text{NO}][\text{O}][\text{M}] - k_5[\text{H}][\text{NO}_2]$$

Therefore

$$([\text{NO}_2]/[\text{NO}])_{ss} = k_9[\text{M}][\text{O}]/k_5[\text{H}]$$

Substituting the exit plane concentrations of M, O, and H, and  $k_5$  and  $k_9$  evaluated at the exit plane temperature in the expression yields

$$[\text{NO}_2]/[\text{NO}]_{\text{exit, steady state}} = 0.6 \times 10^{-5}$$

This result compares favorably with the results of the full computer solution, i.e.,

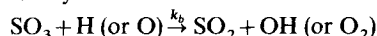
$$[\text{NO}_2]/[\text{NO}]_{\text{exit, finite rate}} = 1.6 \times 10^{-5}$$

#### Oxides of Sulfur

The balance between  $\text{SO}_2$  and  $\text{SO}_3$  is analogous to the one with  $\text{NO}/\text{NO}_2$  discussed previously. The controlling reactions are the homogeneous formation of  $\text{SO}_3$  by the reaction



and its reduction by H or O atoms



A steady-state analysis can be applied as before with  $\text{SO}_2$  replacing NO as the steady-state species. The analysis gives the expression

$$\left(\frac{[\text{SO}_3]}{[\text{SO}_2]}\right)_{ss} = \frac{k_a[\text{M}]}{k_b(1 + [\text{H}]/[\text{O}])}$$

Using rate constants based on Table 1 parameters and nozzle exit properties ( $T = 945^\circ\text{K}$ ), one has

$$([\text{SO}_3]/[\text{SO}_2])_{ss} = 2 \times 10^{-6}$$

Since the destruction reaction has a 10.8 kcal activation energy, the steady-state balance would shift toward  $\text{SO}_3$  at lower temperatures. However, as the wake entrains air and cools, the balance is lost because the H and O atoms recombine. Since the recombinations  $\text{O} + \text{O}_2 + \text{M} \rightarrow \text{O}_3 + \text{M}$ , and  $\text{NO} + \text{O} + \text{M} \rightarrow \text{NO}_2 + \text{M}$ , are much faster than  $\text{SO}_2 + \text{O} + \text{M} \rightarrow \text{SO}_3 + \text{M}$ , the  $[\text{SO}_3]/[\text{SO}_2]$  ratio will tend to be frozen near its very low value in the undiluted exhaust. The role of several other plausible reactions (e.g.,  $\text{OH} + \text{SO}_2 + \text{M} \rightarrow \text{HSO}_3 + \text{M}$ ) cannot be evaluated because no rate data are available.

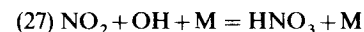
#### CO Oxidation

The phenomenological aspects of CO oxidation have been discussed earlier. Numerical results show that a considerable decrease in CO can occur in the nozzle and jet under low HC conditions. Calculations for the zero HC run, presented in Fig. 2, show that the proportion of CO in the exhaust is decreased from 3000 ppm in the nozzle throat to 2200 ppm at the exit and then is further reduced to 1750 ppm at the tip of the jet core region.

The CO levels for the runs with 500 ppm  $\text{CH}_4$  initially, where CO was again 3000 ppm at the throat, are 2890 ppm at the exit, and 2470 ppm finally. When the portion of  $\text{CH}_4$  was set at 3000 ppm, the corresponding CO levels increase to 3200 ppm and 3380 ppm due to the continuing oxidation.

#### Nitric Acid Formation by $\text{NO}_2$ Oxidation

The possibility for substantial  $\text{NO}_2$  formation in regions of unburned fuel with afterburning raises an accompanying possibility that nitric acid may form downstream



Nitric acid formation was largely discounted in earlier work<sup>30</sup> because no effective mechanism was included for  $\text{NO}_2$  production in the exhaust.

In the sample calculations presented in Figs. 2-4, very little  $\text{HNO}_3$  is observed to form. The  $\text{HNO}_3$  is not thermally stable at the high temperature of the exhaust at maximum power. The equilibrium ratio  $[\text{HNO}_3]/[\text{NO}_2]$  can be computed using the expression

$$[\text{HNO}_3]/[\text{NO}_2] = K_c[\text{OH}]$$

where  $K_c$  is the equilibrium constant for reaction (27) in units of  $\text{cm}^3/\text{mole}$ . With  $[\text{OH}]$  generously estimated to be  $10^{-10}$  mole/ $\text{cm}^3$ , the  $[\text{HNO}_3]/[\text{NO}_2]$  ratio is

$$[\text{HNO}_3]/[\text{NO}_2] = 0.002 \text{ at } 1000^\circ\text{K}$$

$$= 0.03 \text{ at } 900^\circ\text{K}$$

$$= 1.0 \text{ at } 800^\circ\text{K}$$

Hence,  $\text{HNO}_3$  cannot form until the exhaust has begun to cool through entrainment of ambient air, even if  $\text{NO}_2$  is present. At lower power settings with exhaust temperatures below  $800^\circ\text{K}$ , any  $\text{HNO}_3$  formed would be thermally stable in the undiluted plume.

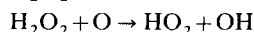
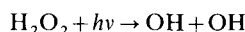
Streamtube calculations in the near jet will probably not indicate substantial  $\text{HNO}_3$  formation because of the difficulty in getting simultaneously high  $\text{NO}_2$  and OH levels which are required. At lower temperatures  $\text{HNO}_3$  is more stable, but so is  $\text{H}_2\text{O}_2$ , and there will be less OH. Based on the concentrations ( $[\text{OH}] = 6$  ppm,  $[\text{NO}_2] = 74$  ppm) at 20-m downstream in Fig. 4, the half time for  $\text{NO}_2$  consumption by reaction (27) is on the order of 100 msec if  $[\text{OH}] = \text{const}$ . Any stoichiometric limitation on the extent of reaction due to the small amount of OH could obviate significant  $\text{HNO}_3$  formation. In the mixing region the initial 6 ppm OH would disappear at rates faster than the 100 msec time frame. The reaction



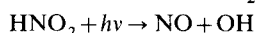
competes with reaction (27), with a half time on the order of 40 msec at the same 20-m position. However, an OH source term might supply OH in the cooling wake as the supply is

used up by reactions (27) and (15) and other OH sink reactions.

The large amounts of  $\text{H}_2\text{O}_2$  and  $\text{HO}_2$  may be candidates for such an OH reservoir<sup>24</sup>



Also, the high levels of NO and OH in streamlines which are free of unburned fuel could lead to significant formation of nitrous acid. Its subsequent photolysis in the wake may then represent an OH source



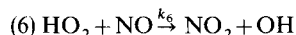
The effect of cross-stream diffusion might be important. Experimental evidence shows that with afterburning some regions of the plume are much richer in unburned HC than others, presumably due to the mode of fuel injection and the configuration of the afterburner. In one set of tests where cross-stream profiles were taken (GE-J85-5) the central regions contained unburned HC.<sup>31</sup> Thus, the chemistry with diffusion may be very complex if there is significant supply of reactants by turbulent diffusion between fuel free streamlines with nominal behavior like Fig. 2 and streamlines which might appear as in Fig. 4. Such a situation in the cooling wake might defy simplification because of the following considerations: 1) OH from zero HC streamlines may mix with  $\text{NO}_2$  from regions containing unburned HC; this is a source of  $\text{HNO}_3$ . 2) The zero HC streamlines also contain H and O which destroy  $\text{NO}_2$ . 3) Streamlines containing  $\text{NO}_2$  also contain HC which can scavenge H and O. 4) Many of the reaction rates are strongly temperature dependent; rates may also be limited by diffusion rather than by kinetics. Therefore, it might be difficult to estimate the extent of conversion of  $\text{NO}_x$  to  $\text{HNO}_3$  in the wake if species migrations across streamlines are important. In that case a fully coupled fluid dynamics/chemistry model would be needed for analysis.

#### IV. Sensitivity of Results to Input Data

A systematic investigation of the sensitivities of computed results to uncertainties in input data may be divided into two categories: 1) sensitivity to rate data, and 2) sensitivity to input species concentrations.

##### Rate Constants

For purposes of illustration, the previous focus on the possibility of  $\text{NO}_2$  formation will be further developed. It is known that the hydroperoxyl radical can rapidly oxidize nitric oxide, as follows:



The value for  $k_6$  listed in Table 1 is probably an upper limit as discussed previously. To ascertain the sensitivity of results to  $k_6$ , the computations shown in Fig. 4 were repeated with  $k_6$  reduced by a factor of 10. The upper limit used in Fig. 4 and the order of magnitude reduction in  $k_6$  band it around the central value of  $1.8 \times 10^{11} \text{ cm}^3/\text{mole sec}$  recently suggested.<sup>24</sup> The  $\text{NO}_2$  level at 20 m showed a concomitant reduction from 76 ppm to 11 ppm. Thus, reaction (6) is a key in calculating the  $\text{NO}_2$  level, with a response sensitivity of about two thirds of the rate constant uncertainty.

##### Sensitivity to Species Concentrations

In the fuel free plume the chemistry is simple enough that less time consuming algebraic methods suffice. One may again focus on  $\text{HO}_2$  because of its potential importance in oxidizing nitric oxide. In many private discussions, it was frequently asserted that high concentrations of hydrogen atoms implied high  $\text{HO}_2$  concentrations because of the following rapid reaction:



The relationship of  $[\text{HO}_2]$  to  $[\text{H}]$  is readily assessed with the help of Table 3, which shows that reactions (21, 22, and 25) define the major formation and destruction processes for  $\text{HO}_2$ . In this event the rate expression is

$$d[\text{HO}_2]/dt = k_{21}[\text{H}][\text{O}_2][\text{M}] - (k_{22} + k_{25})[\text{H}][\text{HO}_2]$$

If  $\text{HO}_2$  is in a steady state, the following equation may be derived:

$$([\text{HO}_2]/[\text{M}])_{ss} = [(k_{21}/(k_{22} + k_{25}))][\text{O}_2]$$

Thus, the  $\text{HO}_2$  concentration is independent of H. This condition obviates the need for a parametric sensitivity study based on uncertainties in the concentrations of hydrogen atoms. Also, it is clear that this equation defines the sensitivity of  $\text{HO}_2$  formation to uncertainties in the rate data for reactions (21, 22, and 25). Hence a parametric study is unnecessary.

#### V. Conclusions

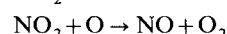
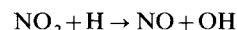
The major conclusions reached in the investigation are as follows:

1) In an afterburning engine, nonequilibrium effects are an important aspect of the chemistry in the engine exhaust expansion nozzle and exhaust jet regime. With relatively low HC emissions there is substantial oxidation of CO to  $\text{CO}_2$  in the nozzle and jet, and the concomitant production of H atoms maintains the concentrations of H, O, and OH well above their equilibrium values. The partial equilibrium of some bimolecular reactions are the basis for useful relationships among the concentrations of H, O, OH, and  $\text{H}_2$ . However, these radicals cannot be related to major species because recombination reactions are far out of equilibrium.

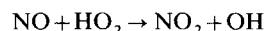
2) Hydrocarbons have a scavenging effect on certain exhaust inorganic radicals. Introduction of HC in quantities of the same order as CO reduces the H and O concentrations by two orders of magnitude and OH by one order of magnitude.

3) Hydrocarbon oxidation steps produce large quantities of  $\text{H}_2\text{O}_2$ ;  $\text{HO}_2$  becomes the dominant radical species.

4) Oxidation of NO to  $\text{NO}_2$  is not significant in the exhaust jet if unburned hydrocarbons are not present. The  $\text{NO}_2/\text{NO}$  ratio is maintained well below its equilibrium value by fast reactions such as



5) With HC present, H and O atoms are low and appreciable amounts of  $\text{NO}_2$  are formed by



6) Oxidation of  $\text{SO}_2$  to  $\text{SO}_3$  is forestalled in a manner exactly similar to the NO- $\text{NO}_2$  system in the absence of unburned fuel.

7) Significant amounts of  $\text{HNO}_3$  do not form in the uncooled exhaust and isothermal core at maximum power.

8) The possibility for significant conversion of  $\text{NO}_x$  to  $\text{HNO}_3$  in the cooling wake cannot be ruled out when unburned fuel is present in the exhaust. In the mixing region,  $\text{H}_2\text{O}_2$ ,  $\text{HO}_2$  and  $\text{HNO}_2$  may serve as OH sources.

#### References

- 1 Abramovich, G. N., *The Theory of Turbulent Jets*, MIT Press, Cambridge, Mass., 1963.
- 2 Forstall, W. and Shapiro, A., "Momentum and Mass Transfer in Co-Axial Gas Jets," *Applied Mechanics*, Vol. 17, 1950, pp. 399-408.
- 3 Bittker, D. A. and Scullin, V. J., "General Chemical Kinetics Computer Program for Static and Flow Reactions, with Application to Combustion and Shock Tube Kinetics," TN D-6586, 1972, NASA.
- 4 Fletcher, R. S. et al., "The Control of Oxides of Nitrogen Emission from Aircraft Gas Turbine Engines, Vol. 1, Program Description and Results," Rept. FAA-RD-71-111, 1, 1971, Federal Aviation Administration, Washington, D. C.



<sup>5</sup> Laurendeau, N., "The Thermal Decomposition of Nitric Oxide and Nitrogen Dioxide," Rept. TS-72-4, April 1972, Univ. of California at Berkeley, Berkeley, Calif.

<sup>6</sup> Garvin, D. and Gevantman, L. H., "Chemical Kinetics Data Survey III, Selected Rate Constants for Chemical Reactions of Interest in Atmospheric Chemistry," NBS Rept. 10-867, June 1972, U.S. Dept. of Commerce, Washington, D.C.

<sup>7</sup> Davis, D. D., private communication, Sept. 12, 1972, Univ. of Maryland, College Park, Md.

<sup>8</sup> Kondratiev, V. N., *Rate Constants of Gas Phase Reactions*, Office of Standard Reference Data, National Bureau of Standards, Washington, D.C., June 1972.

<sup>9</sup> Baulch, D. L. et al., *High Temperature Reaction Rate Data*, No. 5, School of Chemistry, The Univ. of Leeds, Leeds, England, July 1970.

<sup>10</sup> Baulch, D. L. et al., *High Temperature Reaction Rate Data*, No. 4, School of Chemistry, The Univ. of Leeds, Leeds, England, Dec. 1969.

<sup>11</sup> Wilson, W. E., "A Critical Review of the Gas-Phase Reaction Kinetics of the Hydroxyl Radical," *Journal of Physics and Chemical Reference Data*, Vol. 1, No. 2, 1972, pp. 535-573.

<sup>12</sup> Baulch, D. L. et al., *Evaluated Kinetic Data for High Temperature Reactions*, Butterworths, London, England, 1972.

<sup>13</sup> Lloyd, A. C., "Evaluated and Estimated Kinetic Data for the Gas Phase Reactions of the Hydroperoxyl Radical," NBS Rept. 10447, 1971, U.S. Dept. of Commerce, Washington, D.C.

<sup>14</sup> Morely, C. and Smith, I. W. M., "Rate Measurements of Reactions of OH by Resonance Absorption," *Journal of The Chemical Society Faraday Transactions*, Vol. II, 1972, p. 68.

<sup>15</sup> Levy, A. et al., "Mechanisms of Formations of Sulfur Oxides in Combustion," *Environmental Science and Technology*, Vol. 4, Aug. 1970, pp. 653-662.

<sup>16</sup> Garvin, D., ed., "A Compendium of Evaluated and Estimated Rate Coefficients," NBS Rept. 9884, July 1968, U.S. Dept. of Commerce, Washington, D.C.

<sup>17</sup> Herron, J. T. and Huie, R. E., "Rate Constants for the Reactions of Atomic Oxygen ( $O^3P$ ) with Organic Compounds in the Gas Phase," unpublished, 1972, National Bureau of Standards, Washington, D.C.

<sup>18</sup> Hecklen, J., "Gas Phase Reactions of Alkylperoxy and Alkoxy Radicals," *Advances in Chemistry*, Vol. 76 II, 1968, p. 23.

<sup>19</sup> Demerjian, K. L., Kerr, J. A., and Calvert, J. G., "The Mechanism

of Photochemical Smog Formation," Typescript, 1972, Ohio State Univ., Columbus, Ohio; to appear in *Advances in Environmental Science and Technology*, Vol. 4, 1974.

<sup>20</sup> Johnston, H. S., "Gas Phase Reaction Kinetics of Neutral Oxygen Species, NSRDS-NBS 20, Sept. 1968, National Bureau of Standards, Washington, D.C.

<sup>21</sup> Garvin, D. and Gevantman, L. H., "Chemical Kinetics Data Survey, III. Selected Rate Constants for Chemical Reactions of Interest in Atmospheric Chemistry," NBS Rept. 10-867, June 1972, U.S. Dept. of Commerce, Washington, D.C.

<sup>22</sup> Hampson, R. F., ed., "Chemical Kinetics Data Survey, I. Rate Data for Twelve Reactions of Interest for Stratospheric Chemistry," NBS Rept. 10-692, Jan. 1972, U.S. Dept. of Commerce, Washington, D.C.

<sup>23</sup> Schofield, K., "A Scientific Report on Evaluated Chemical Rate Constants for Various Gas Phase Reactions," Rept. TR-71-57, Dec. 1971, Delco Electronics, General Motors Corp., Santa Barbara, Calif.

<sup>24</sup> Dept. of Transportation Climatic Impact Assessment Program, "The National Stratosphere, 1974," *CIAP* Monograph, Vol. 1, third preliminary working draft, updated to May 1973 (not yet released).

<sup>25</sup> McGregor, W. H. et al., "Concentration of OH and NO in YJ93-GE-3 Engine Exhausts Measured in Situ by Narrow-Line UV Absorption," Second Conference on the Climatic Impact Assessment Program, Nov. 14-17, 1972, U.S. Dept. of Transportation, Washington, D.C.

<sup>26</sup> Forney, A. K., "Engine Exhaust Emission Levels," *Journal of Aircraft*, Vol. 10, No. 12, Dec. 1973, pp. 717-720.

<sup>27</sup> Bradley, J. N., *Flame and Combustion Phenomena*, Methuen, London, England, 1969.

<sup>28</sup> Williams, M. R., private communication, Bristol Engine Div., Rolls-Royce, Bristol, England, July 2, 1973.

<sup>29</sup> Diehl, L. A., "Measurement of Gaseous Emissions from an Afterburning Turbojet Engine at Simulated Altitude Conditions," TM X-2726, March 1973, NASA.

<sup>30</sup> Anderson, L. B. et al., "Turbojet Exhaust Reactions in Stratospheric Flight," AIAA Paper 73-99, Washington, D.C., 1973.

<sup>31</sup> Dept. of Transportation Climatic Impact Assessment Program, "Nature of Propulsion Effluents," *CIAP*, Vol. 2, updated to March 1973 (not yet released).